Surface Roughness and Material Removal Rate of Lapping Process on Ceramics

Yoomin Ahn* and Sang-Shin Park**

(*Received September 2, 1996*)

Lapping is a widely used surface finishing process for ceramics. An experimental investigation is conducted into the lapping of alumina, Ni-Zn ferrite and sodium silicate glass using SiC abrasive to study the effect of process parameters, such as abrasive particle size, lapping pressure, and abrasive concentration, on the surface roughness and material removal rate during lapping. A simple model is developed based on the indentation fracture and abrasive particle distribution in the slurry to explain various aspects of the lapping process. The model provides predictions for the surface roughness, R_a and R_t, on the machined surface and rough estimation for the material removal rate during lapping. Comparison of the predictions with the experimental measurements reveals same order of magnitude accuracy.

Key Words: Lapping, Surface Finishing Process, Abrasive, Surface Roughness, Material Removal Rate

1. Introduction

Lapping is generally used after grinding process to make ceramic materials satisfy the required size tolerance and surface roughness. The usual method of lapping process is to rub the workpiece against a lapping wheel with abrasive particles between them. In lapping a metallic block such as cast iron or tin is used as the lapping wheel. Abrasive particles which are commonly used include diamond, SiC, Al_2O_3 and boron carbide. Lapping process on ceramics usually produces the surface finish as about $1 \sim 0.01$ μm of R_a. The abrasive machining mechanism of lapping on brittle ceramics is to be much different from on metals which are deformed plastically well. It is well known by experimental researches (Grimes, 1977 and Marshall, 1983) that the lapping on ceramics are performed by brittle fracture rather than plastic deformation. Cracks are generated by the mechanical contact between workpiece and abrasive particles and the stock removal of workpiece was mostly done by lateral one among the cracks. The abrasive particles of each grit grade have a size deviation approximated to normal distribution. Therefore, only a few of or some large ones among the abrasive particles which exist between workpiece and lapping wheel are squeezed enough to cause cracks on the contact surface of workpiece (Imanaka, 1966).

An early study aimed at predicting the roughness generated on lapped surfaces of brittle materials is that of Imanaka (1966). Imanaka derived an equations for the roughness of lapped surface which took into the account of the distribution of grain diameters in the abrasive slurry. The model is based on the assumption that an individual abrasive grain acts like a spherical indenter producing Hertzian cone cracks in the materials. Material removal was somehow attributed to the cone cracks breaking open to be the surface and the maximum depth of the cone cracks was assumed to be the surface roughness. However this model can not explain the presence of residual stresses and plastic deformation on the lapped surface, because it is found that the indentation stress field under blunt indenters such as a sphere

* Dept. of Mechanical engineering, Hanyang University

** Turbo Power Machinery Research Center, Seoul National University

is essentially elastic up to the point of fracture (Lawn, 1975). If material removal were accomplished due to indentations by sharp (e. g. Vickers, conical) indenters, the finished surface would show evidence of plastic deformation (Cook, 1990). Chauhan et al. (1993) developed a model for the free abrasive machining of ceramics based on indentation fracture by sharp indenter. The model was reasonably good in predicting the surface finish and depth of the plastically deformed layers on free abrasive machined surface. In recent studies, the material removal rate as well as surface roughness are predicted by Buijs et al. (1993). Their model is based on fracture indentation theory and it is assumed that material removal is caused by rolling abrasive particles. In this paper we refined the analysis of Chauhan's model and developed more rigorous lapping model by including the phenomena of abrasive grain fracture. The surface roughness and material removal rate (MRR) are predicted by the developed model and are compared with experimental results.

2. The Indentation Model for Lapping

2.1 Material removal mechanism

The proposed lapping model as that of Chauhan et al. (1993), is based on the fact that machining is carried out by the microscopic action of abrasive particles which are loaded against the work surface. By considering a suitable superposition of these microscopic indentation events, it should, in principle, be possible to predict material removal rate, surface roughness, the number of active (cutting) particles, and the load acting on individual abrasive particles during the lapping process. The model relies on lateral cracks as the cause of material removal. It is well observed that a lateral crack is typically produced by a sharp indenter (Vickers, cone) in a brittle solid as shown in Fig. 1(b) (Lawn, 1975). The depth at which the lateral crack originates under a sharp indenter is usually about the same as the maximum depth of the plastic zone under the indentation. During quasi-static indentation, such lateral cracks usually propagate during unloading of the indenter, almost parallel to the surface before intersecting the surface (Cook, 1990). This causes a sliver of material to be removed. The depth of the material removed is therefore roughly equal to the plastic zone depth. It is assumed that such well developed lateral cracking occurs in the ceramic workpiece under the sharp abrasive particle contacts (indentations) and that the action of the abrasive particle is similar to the action of a hard, rigid, and sharp indenter indenting a brittle solid.

Support for this mode of material removal in lapping is based on microscopic observations of highly polished surfaces of brittle materials which have been subsequently subjected a lapping process for short time periods (Chauhan, 1993). The

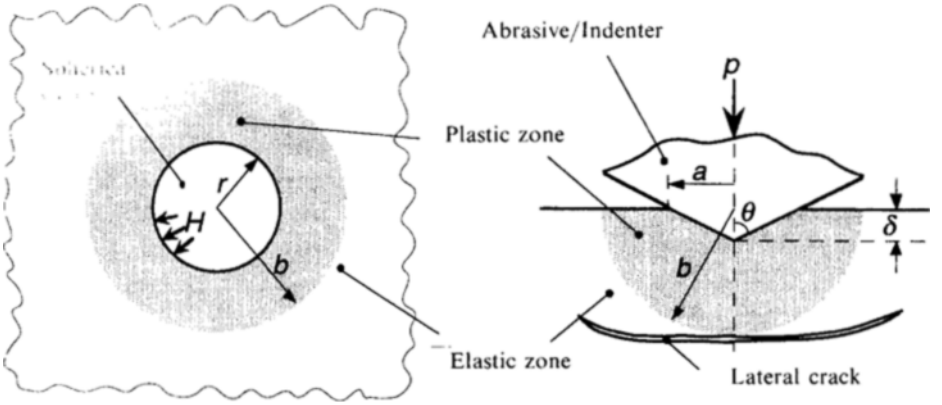

(a) Expanding spherical cavity in an infinite elastic-plastic solid

(b) Indentation with associated hemispherical plastic zone

Fig. 1 Spherical cavity model of Hill

surface is seen to be marked by numerous quasi-static and sliding type of indentations and lateral cracking such as those typically generated by conical or pyramidal indenters. Similar observations have been made by Grimes *et al.* (1977), Marshall *et al.* (1983), and Ajayi and Ludema (1988). Furthermore, the presence of plastically deformed layers on lapped surfaces of ceramics suggest that the sharp indentation model is a better assumption than one based on indentation with blunt (e. g. spherical) indenters.

It is assumed that heat generation at the abrasive-workpiece interface and interaction between the abrasive particles can be neglected. Active particles are identified as those abrasive particles which actually participate in the cutting process. Using a statistical description of the abrasive particles in the slurry and on the workpiece surface, the number of active (cutting) abrasive particles and the distribution of load amongst active abrasive particles are estimated. From an estimate of the maximum indentation depth of an abrasive particle, the maximum depth at which a lateral crack occurs (=maximum plastic zone size) is obtained. The plastic zone will be assumed to be hemispherical in shape with radius b as shown in Fig. 1(b).

The expanding spherical cavity analysis, originally proposed by Hill (1985) and semi-experimentally modified by Marsh (1964), can be used to obtain an approximate estimate of the plastic zone size as a function of the indentation volume, indenter geometry, and H/E, where H is the mean contact pressure (hardness) under the indenter and E is the Young's modulus of the solid. For a spherical cavity of radius r in an infinite elastic-plastic solid expanding under internal pressure, H (Fig. 1(a)), the following equations provide a relation between H/E and the ratio of plastic zone radius (b) to cavity radius (r) (Hill, 1985).

$$\left(\frac{b}{r}\right)^3=\frac{E}{3(1-v)\,Y} \tag{1}$$

$$\frac{H}{Y}=0.28+\frac{1.8}{3-\alpha}ln\frac{3}{\alpha+3\beta-\alpha\beta} \tag{2}$$

where $\alpha=(1-2v)\frac{Y}{E}$, $B=(1+v)\frac{Y}{E}$, and v is Poisson's ratio of the solid.

Eliminating Y, yield strength which is difficult to obtain for brittle material, from Eqs. (1) and (2), we get

$$\frac{3(1-v)H}{E\left(\frac{r}{b}\right)^3}-\frac{1.8}{3-\frac{(1-2v)}{3(1-v)}\left(\frac{r}{b}\right)^3}\cdot ln\frac{3}{\frac{(4+v)}{3(1-v)}\left(\frac{r}{b}\right)^3-\frac{(1-2v)(1+v)}{9(1-v)^2}\left(\frac{r}{b}\right)^6}=0.28 \tag{3}$$

It had been proposed by Marsh (1964) that the indentation process in a brittle material can be modelled using Hill's expanding spherical cavity analysis. In this model, the loading of the indenter on to the solid with a certain mean contact pressure is analogous to a cavity under pressure. Then a relationship between cavity radius, r, and indentation radius, a, is found by assuming that the volume of the indentation impression is equal to the volume of the cavity. This gives

$$\left(\frac{r}{a}\right)^3=\frac{\cos\theta}{\varphi} \tag{4}$$

where φ depends on the geometry of the indenter. For a conical indenter, $\varphi=2$ and for a pyramidal indenter, $\varphi=\pi$, Using the value of r from Eq. (4), the ratio of plastic zone radius to indentation radius, $\xi(=b/a)$ can be written as

$$\xi=\left(\frac{b}{r}\right)\left(\frac{\cos\theta}{\varphi}\right)^{\frac{1}{3}} \tag{5}$$

The mean contact pressure applied by the indenter on the specimen surface, H, is insensitive to indenter or abrasive grain geometry (Marsh, 1964). If P_i is the load applied on a grain, then

$$H=\frac{P_i}{\Psi a^2} \tag{6}$$

where $\Psi=\pi$ for a conical indenter and $\Psi=2$ for a pyramidal indenter. For a sharp indenter, the depth of penetration (δ) into the solid due to an applied load P_i is $a/\tan\theta$. Therefore Eq. (6) can be rewritten as

$$P_i=\Psi H(\tan^2\theta)\,\delta^2 \tag{7}$$

In the lapping of ceramics, the externally applied lapping load P is transmitted to the workpiece at the microscopic contacts between

the workpiece and the abrasive particles. At any given instant if there are n abrasive particles participating (active) in the cutting action, then

$$P=\sum_{i=1}^{n} P_i \tag{8}$$

where P_i is the load carried by the ith abrasive particle, P is the total externally applied lapping load, and n is the total number of active particles. Note that the load P_i on each abrasive particle can vary depending on its size.

2.2 Calculation of surface roughness and material removal rate

The abrasive slurry used in lapping consists of abrasive particles suspended uniformly in a vehicle (lapping liquid). Let m denote the abrasive concentration of slurry which is defined as

$$m=\frac{Mass\ of\ the\ abrasive}{Mass\ of\ the\ lapping\ liquid} \tag{9}$$

The abrasive particles are not all of the same size (diameter). The particle size has some distribution, often assumed to be a normal distribution with some mean diameter d and standard deviation σ. Both of these can be measured and are often provided by the manufacturer. These parameters allow the total number of abrasive particles, N, trapped between the workpiece surface and the lapping block (rotating wheel) to be estimated as follows: Of these N particles, only a fraction are expected to be cutting at any given instant of time.

It is assumed that all particles with diameters up to the diameter of the largest particle (X_L) in a sample are accommodated between rotating lapping block and workpiece, and the gap between them are X_L. The total number of particles in a volume AX_L is obtained as (Imanaka, 1966)

$$\begin{aligned} N&=\frac{AX_L}{4/3\pi(d/2)^3}\left(\frac{V}{V'+V}\right)\\ &=\frac{6A(d+\lambda\sigma)}{\pi(d)^3}\left(\frac{m\rho'}{\rho+m\rho'}\right) \end{aligned} \tag{10}$$

where A is the surface area of the workpiece, V and ρ is the total volume and density of the abrasive, respectively, V' and ρ' is the total volume and density of the lapping liquid, respectively, and λ is the ratio of the half range (half of the difference between the largest particle size and the smallest particle size) to the standard deviation (σ) of the sample. From this

$$X_L=d+\lambda\sigma \tag{11}$$

where, λ, of course, depends on the sample size under consideration.

A relationship between λ and sample size N can be obtained from simulation experiments on the distribution curve which represents the abrasive particle size distribution curve. A number of such simulation experiments were carried out on standardized normal distribution curve (assumed to approximate the actual abrasive particle size distribution) using a random sampling procedure. From the simulation results, the following relationship between λ and N was derived using a regression analysis

$$\lambda=1.5468(\log N)^{0.64935} \tag{12}$$

The values of λ and N can be solved by Eqs. (10) and (12).

Let X be the distance between the lapping block and the workpiece surface. The value of X will be estimated from knowledge of lapping parameters. It is reasonable to assume that only those abrasive particles having a diameter x greater than X will cause material removal. This defines the set of active particles. Since it is assumed that all of the abrasive particles are sharp indenters (apical angle$=2\theta$), if P_i is the load on the ith active particle with diameter x_i and δ_i is the depth of penetration into the workpiece and δ_i' is the depth of penetration into the lapping wheel then from Eq. (7),

$$P_i=\Psi H(\tan^2\theta)\,\delta_i^2=\Psi H'(\tan^2\theta)\,\delta_i'^2$$
$$\delta_i+\delta_i'=x_i-X$$

Here H is the workpiece hardness and H' is the lapping wheel hardness. Eliminating δ_i and δ_i' from these two equations, we get

$$P_i=\frac{\Psi H(\tan^2\theta)}{(1+\sqrt{H/H'})^2}(x_i-X)^2 \tag{13}$$

Using Eq. (13) as the force indentation relationship implies that interaction among abrasive particles is neglected. Using Eq. (13) and the probability density function, $\phi(x)$, describing the abrasive particle size distribution, the discrete

sum in Eq. (8) is to be well approximated as

$$P=\frac{\Psi H(\tan^2\theta)N}{(1+\sqrt{H/H'})^2}\int_X^{X_L}(x-X)^2\phi(x)\,dx \quad (14)$$

where N is the total number of particles present on the workpiece surface. Abrasive particles are assumed as so rigid that the deformation of them are negligible. However, the particle is to be crushed by fracture if compression load is increased over the critical strength of grain. In solving of Eq. (14), if large particles are compressed under the load more than critical strength, the largest particle size, X_L, must be reduced by using Eq. (13).

The expected number of active particles will be

$$n=N\int_X^{X_L}\phi(x)\,dx \quad (15)$$

Also, the maximum load on a single particle is

$$P_{\max}=\frac{\Psi H(\tan^2\theta)}{(1+\sqrt{H/H'})^2}(X_L-X)^2 \quad (16)$$

and the mean load on a single particle will be given by

$$P_{avg}=P/n \quad (17)$$

Similarly, we find the expected total area of contact as

$$A=P/H \quad (18)$$

If we assume that the thickness of the material above the lateral crack plane is equal to the depth of the plastic zone as stated earlier, then since largest particle would produce a lateral crack at the greatest depth, the peak-to-valley surface roughness (=largest plastic zone depth, $b_{\max}$) is

$$R_t=\xi a_{\max}=\xi\tan\theta\delta_{\max}=\xi\frac{\tan\theta}{(1+\sqrt{H/H'})}(X_L-X) \quad (19)$$

and the arithmetic average surface roughness is

$$R_a=\frac{\xi\tan\theta\frac{N}{n}}{(1+\sqrt{H/H'})}\int_X^{X_L}(x-X)\,\phi(x)\,dx \quad (20)$$

Even though the precise prediction of material removal rate (MRR) is very difficult to obtain, the lower bound of MRR can be estimated. It is assumed that workpieces do not move during lapping and rolling contacts are only occurred between workpiece and lap. By assuming that the number of indenting points per particles to be four during one self revolution (Buijs, 1993) and the removed volume by rolling contact of active particle is equal to the plastically deformed zone with the shape of half hemisphere, the material removed depth per unit time is

$$MRR_{\min}=\frac{8\pi DSN(\xi\tan\theta)^3}{3A}\int_{x}^{X_L}\frac{(x-X_L)^3}{x}\phi(x)\,dx \quad (21)$$

where S is the rotational speed of lapping wheel and D is the average diameter of turning circles of active particles around the center of lapping wheel. In fact, the workpiece within retaining ring is usually rotating during lapping. Hence the real number of rolling contacts must be different from the one estimated in Eq. (21). Real material removal rate should be greater than $MRR_{\min}$. The material stock removed by sliding contacts, which take a shape of about half cylinder, could be greater than that by rolling contacts. In lapping process, the more sliding contacts happens, the greater amount of materials are really removed than $MRR_{\min}$ calculated from Eq. (21).

3. Lapping Experiments and Analytical Estimations

A computer program was written to calculate the surface roughness and material removal rate. The result of lapping experiments are compared with the model predictions. The workpiece materials examined experimentally were aluminum oxide, Ni-Zn ferrite, and sodium-silicate glass while the abrasive grain material was SiC. Their properties are given in Table 1. Water was used as the vehicle for the abrasive. The experiments were conducted on a Model 12 Free Abrasive Machine manufactured by SPEEDFAM Corporation. The machine had a variable speed option for rotating lapping wheel. However, the operator cannot control the rotating speed of workpiece which is governed by the friction between workpiece and lap. A hardened steel (HRC=60) block of 0.3 m

Table 1 Mechanical properties of workpiece material and abrasive power

Properties	Alumina	Ni-Zn ferrite	Glass	SiC
Density (g/cc)	3.92	5.30	2.42	3.2
Vickers hardness(kg/mm^2)	1540	6.75	571	2600
Elastic modulus(GPa)	352	180	65	440
Poisson's ration	0.23	0.20	0.17	0.17
Compressive strength(MPa)	—	—	—	2500

Table 2 Lapping process conditions.

Lapping wheel speed	60.0 rpm
Lapping time	10.0 min
Lapping pressure	7, 14, 17, 21, 24 kPa
Grit # of abrasive	#1000, #600, #400, #320, #240
Abrasive concentration	0.1, 0.25, 0.4

diameter was used as lapping wheel. Spacers were used to separate the individual workpieces in the retaining ring. The lapping process conditions of experiments are listed in Table 2. A profilometer, Talyform-50, manufactured by Rank-Taylor Hobson was used to measure the surface roughness. Material removal rate was obtained from measurements of weight loss on the workpiece using electronic balance with the resolution of 1 mg. For more details about experiments, refer to Ahn and Han (1993).

One of the inputs to the program is the mean included angle 2θ(mean apical angle) of the abrasive particles. An estimate of the angle 2θ was obtained by measuring the angles (obtuse) from SEM photographs of silicon carbide abrasive powder. The mean value obtained from measurements by Chauhan (1992) is 122° degrees. The standardized probability distribution (Fig. 2) of the particle size of silicon carbide was obtained from the sizing curves supplied by the manufacturer of silicon carbide, who obtained these curves based on the alcohol sedimentation method. Table 3 gives the particle size distribution parameters for each grade of silicon carbide abrasive as derived from the sizing curves by using a software package for fitting Johnson

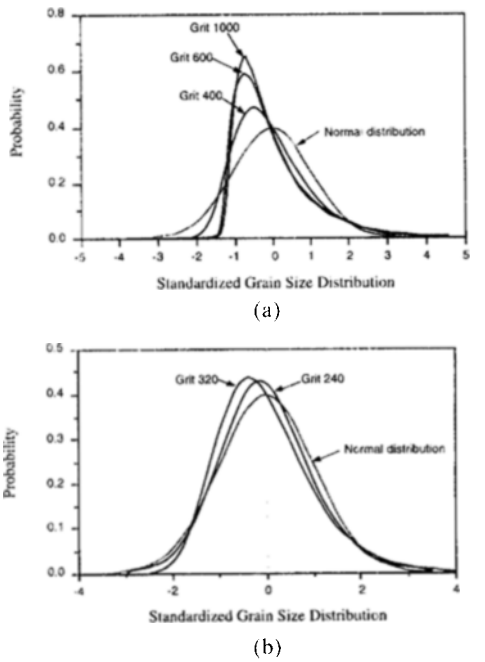

Fig. 2 Standardized probability density distribution of SiC abrasive particle sizes: (a) Grit size 1000, 600, and 400, (b) Grit size 320 and 240.

distributions to univariate data sets (Venkartraman 1988). Figure 2 shows that the measured distribution of abrasive particle sizes approaches a normal distribution for larger grain sizes. In simulation, the abrasive particle size distribution, $\phi(x)$, is assumed as normal distribution. It is expected that simulation results for grain sizes of 22.9, 31.5, and 62.9 μm will therefore be more reliable than those obtained for grain sizes of 6.4 and 14.7 μm, because the skewness and kurtosis of the distribution for grain sizes of 6.4 and 14.7 μm is further deviated from the normal distribution (skewness=0, kurtosis=3) than for grain sizes of 22.9, 31.5, and 62.9 μm.

Table 3 Abrasive powder statistics

Grit #	1000	600	400	320	240
Grain size (μm)	6.400	14.70	22.90	31.50	62.90
Mean (μm)	9.445	13.94	24.10	31.91	52.94
Std. Dev. (μm)	6.599	7.457	9.121	10.66	12.90
Skewness	1.776	1.657	1.203	0.833	0.375
Kurtosis	7.113	6.221	5.479	4.339	3.904
λ_{max} (manufacturer)	3.721	3.495	3.388	3.104	2.873

The main steps involved in the computational procedure are:

1. The value of ξ is calculated by Eqs. (3) and (5), which will be used for the estimation of surface roughness.
2. The values of N and λ are obtained by solving Eqs. (10) and (12). The obtained value of λ is checked to see if it is not greater than the maximum value, λ_{max}, which is controlled by manufacturer.
3. From the knowledge of λ and d, the largest size (X_L) of the abrasive particle present on the work surface is estimated. An iterating procedure is used to obtain the value of X from Eq. (14) for the given value of P. Whenever new X is generated during the iteration procedure, the number of abrasive particles, N, is recalculated by setting X_L (*gap size*) $=X$ in Eq. (10).
4. The value of X is then used to calculate the number of active particles, n, using Eq. (15).
5. Finally, Eqs. (19), (20) and (21) are used to estimate the peak-to-valley (R_t), arithmetic average (R_a) surface roughness and the low bound of material removal rate (MRR_{min}).

The contact between abrasive particle and workpiece is assumed to arise out of a pyramidal indentation. The lapping block is assumed to be perfectly rigid. The nominal lapping pressure is defined as the load acting on unit area of the workpiece surface assuming that it is uniformly distributed. The workpiece area was assumed to be 1000 mm^2 in the calculations even though the actual workpiece area ranged from 500 mm^2 upto 2500 mm^2 in the experiments. The calculations showed that the surface roughness, R_a and R_t, varied little with change in the area (in the range of 10~100000 mm^2) The value of D in Eq. (21) is assumed as the middle, 0.18 m, of outer and inner diameter of wheel. In all of the computations carried out in computational step 2, λ was always greater than λ_{max}. Hence, in the analysis, λ was set equal to λ_{max}. Currently no reliable data for the compressive strength of SiC grain is available. We roughly assumed this value as about 0.3 times of bulk compressive strength of SiC. If we notice irregular shape of abrasive, the assumed value is thought to be reasonable such that the strength of grain is a little less than that of bulk. It is also assumed that the grain fracture occur in cross section area at the middle of grain rather than at the contact points by the size effect and that even though the crushing occurs, the size of abrasive particles take the normal distribution.

4. Results and Discussion

4.1 Effect of abrasive particle size

Figures 3, 4 and 5 show respectively the variation of the arithmetic average, R_a, and the peak-to-valley, R_t, surface roughness parameters and MRR with abrasive (SiC) grain size for the three ceramics. The figures show both the experimental results and the analytically calculated values when lapping pressure is 14 kPa and abrasive concentration is 0.25. Not only are the predicted values for R_a and R_t of about the same magnitude of those measured experimentally, but the variations in R_a and R_t with grain size are also well described by the model. The good agreement between the experimentally measured values of surface roughness and the corresponding esti-

mates for R_a and R_t derived from the lapping model provide support for our calculations of the

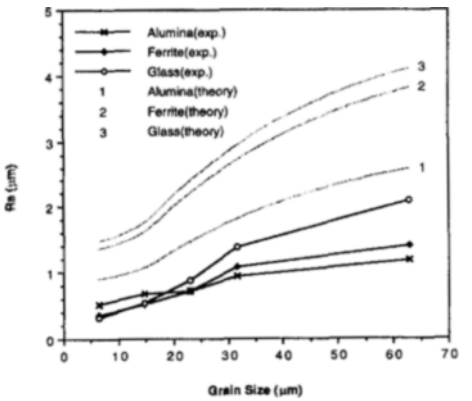

Fig. 3 Variation of R_a with grain size. (pressure = 14 kPa, concentration = 0.25)

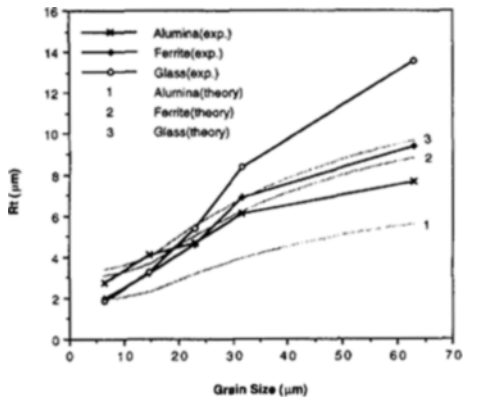

Fig. 4 Variation of R_t with grain size. (pressure = 14 kPa, concentration = 0.25)

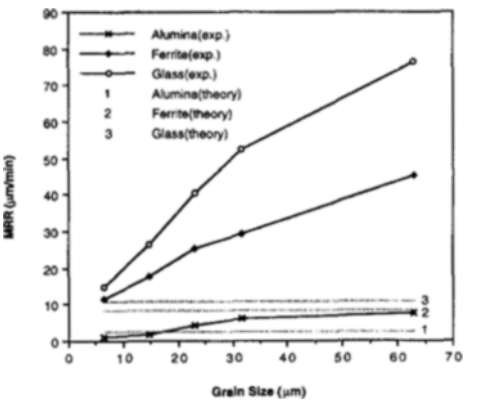

Fig. 5 Variation of MRR with grain size. (pressure = 14 kPa, concentration = 0.25)

number of active particles and the load distribution amongst these particles. Meanwhile, the prediction of lower bound of material removal rate is good at small grain size but that is too low compared to experimental results at large grain size.

The increase in surface roughness with increasing abrasive particle size can be explained qualitatively. For a given slurry concentration and lapping pressure, the number of active particles should be decreased as the particle size is increased. Therefore, the maximum and average loads per particle increases with increasing particle size. Consequently, a deeper indentation of the abrasive particle into the workpiece occurs causing lateral cracks at greater depths. Hence R_a and R_t would be expected to increase with increasing particle size. The increase in material removal rate may be attributed to the same cause if it is assumed that the increased load per particle dominates any reduction in the number of active particles. The estimation for material removal rate with large grain size is seemed to be underestimated by the fact that the number of rolling contacts of abrasives get reduced as the size of grain is increased. However, the removed volume of workpiece by large single grain is to be bigger than that by small single grain. The material removal rate by sliding contacts of abrasive should be much bigger with large grain size than with small one. The underestimation at large grain way be explained by the fact that the material removal rate by sliding contacts is not counted in calculation of MRR_{min}.

4.2 Effect of lapping pressure

Figures 6, 7 and 8 show the experimentally measured variation of R_a, R_t, MRR with lapping pressure for the three ceramics when lapping with a 31.5 μm SiC slurry of 0.25 concentration. In Figs. 6 and 7, surface roughness shows a slight increase with increasing lapping pressure in each of the ceramics in low pressure range; but beyond a threshold value of the lapping pressure surface roughness decreases as lapping pressure increases. The threshold value of the lapping pressure is between 21 and 24 kPa for glass and ferrite and

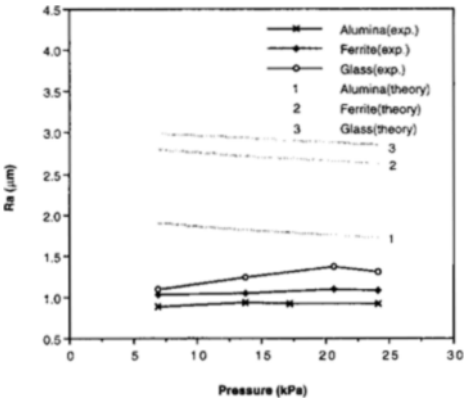

Fig. 6 Variation of R_a with pressure. (grain size= 31.5 m, concentration=0.25)

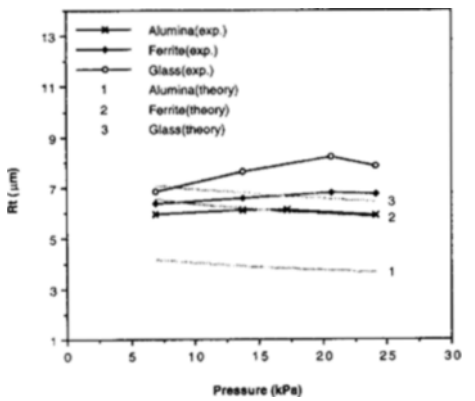

Fig. 7 Variation of R_t with pressure. (grain size= 31.5 m, concentration=0.25)

between 14 and 17 kPa for alumina. This transition in surface finish versus lapping pressure behavior has been attributed to crushing of the SiC abrasive particles when the externally applied pressure exceeds the compressive strength of the abrasive (Chauhan, 1993). The material removal rates continuously increased with lapping pressure in the experiments, see Fig. 8. There was, however, a small but significant change (decrease) in the slope of the *MRR* vs. lapping pressure curves for ferrite and glass with the onset of crushing of the abrasive particles.

The variation of R_a and R_t with lapping pressure as predicted by our analysis is also shown in Figs. 6 and 7. The agreement with experiment is quite good except the trend. In predictions, the values of surface roughness show

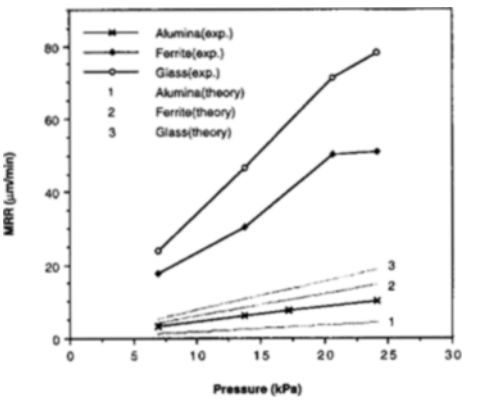

Fig. 8 Variation of *MRR* with pressure. (grain size =31.5 μm, concentration=0.25)

continuous slight decrease. The crushing of the abrasive particles occurred analytically at lower lapping pressure compared to experimental results. The estimation of *MRR* shows good agreement with the experimental result as shown in Fig. 8.

The variation in surface roughness and *MRR* with lapping pressure can be qualitatively analyzed by considering the load on an individual particle. As the lapping pressure is increased, the mean load on an individual abrasive particle would be expected to increase. This is also predicted by the model. Consequently, the *MRR* increases along with R_a and R_t as lapping pressure increases. When the pressure increases beyond a critical value that abrasive particles in the slurry undergo fragmentation, the mean size of an abrasive particle would now decrease. What we have subsequently is a slurry with much finer abrasive particles. Therefore, the surface finish improves as the lapping pressure is increased beyond the threshold limit for onset of crushing.

4.3 Effect of abrasive concentration in the slurry

Preliminary experiments have been conducted to investigated the effect of abrasive particle concentration on surface roughness and material removal rate. The experiments were carried out with 62.9 μm SiC abrasive and at a lapping pressure of 14 kPa. Figures 9 and 10 describe the variation of R_a and R_t with concentration (m) as

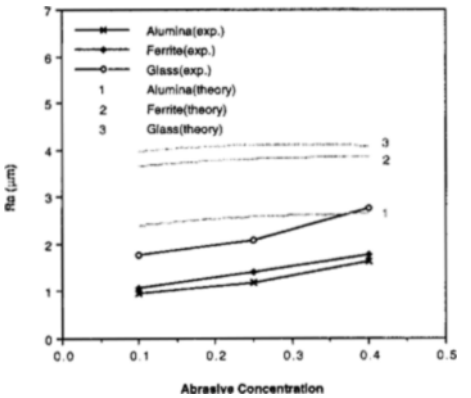

Fig. 9 Variation of R_a with abrasive concentration (m). (grain size=62.9 μm, pressure=14 kPa)

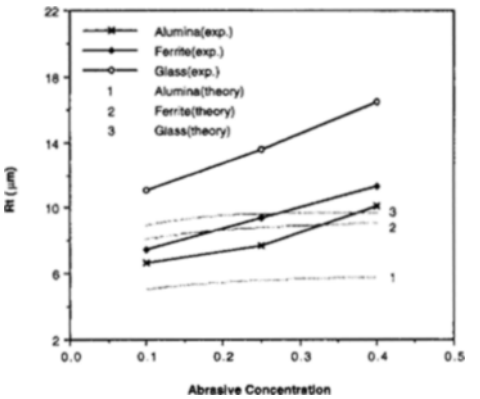

Fig. 10 Variation of R_t with abrasive concentration (m). (grain size=62.9 μm, pressure=14 kPa)

measured in the experiments. Both R_a and R_t were found to increase with increasing of m in the experiments. The predicted trend shows good agreement with the experimental results. This is consistent with the fact that as m decreases, the mean load on an abrasive particles would increase and the largest grain size get smaller by grain fracture. Therefore, the surface finish get smoother with finer grains.

The change of material removal rate with the variation of abrasive concentration is shown in Fig. 11. Experimental result shows that *MRR* is increasing as concentration get dense. This is because the less material is removed as smaller abrasive particles are involved at lapping process

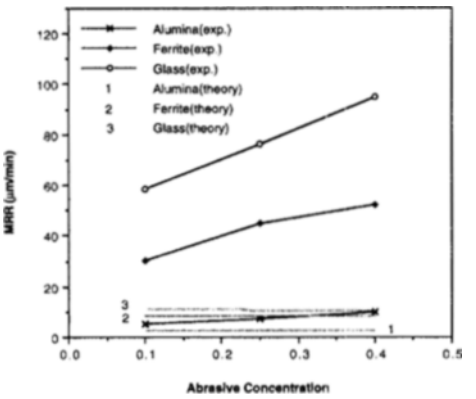

Fig. 11 Variation of *MRR* with abrasive concentration (m). (grain size=62.9 μm, pressure=14 kPa)

when the concentration is low. The estimation for MRR_{min} is significantly low at high concentration. The mean size of active grains should be bigger at high concentration than at low concentration. Therefore, lapping model provides underestimated MRR_{min} at high concentration because the material removed by sliding contacts, which is excluded in MRR_{min}, gets significant at large grain size as explained in Sec. 4.1.

5. Conclusion

Microscopic observations of lapped surfaces of ceramics show that material removal is caused by lateral cracking due to a combination of quasi-static and sliding microindentation applied to the ceramic workpiece by abrasive particles. Based on such observations a simple model, developed by Chauhan et al. to analyze the lapping process, is extended and refined, and used to predict the surface roughness and the material removal rate. The predictions of the model show, except for some cases in *MRR*, reasonable degree of agreement with the experimental observations of the lapping of aluminum oxide, sodium-silicate glass, and Ni-Zn ferrite using SiC abrasive slurry. The experimental and analytical results of this study provide useful insights into the effect of process parameters on lapping performance on ceramics as follows;

(1) The value of surface roughness and material removal rate increase with increasing of the grain size.
(2) As the lapping pressure are increasing, the material removal rate also increases and the surface roughness get slightly worse.
(3) If the abrasive concentration of lapping liquid is increased, lapped surface get coarse and material removal rate is increased.

There are several aspects of further worth of the study for the lapping process. First of all, an experimental work to obtain compressive strength of abrasive SiC grain is required. In order to estimate the material removal rate more precisely, it is needed to analyze the stock removal by sliding contacts of abrasive on workpiece and the rotation of workpiece within the retaining ring.

Acknowledgement

This study was supported by Korea Ministry of Education through Mechanical Engineering Research Fund ME96-E-39. This financial support is gratefully acknowledged.

References

Ahn, Y. and Han, D. C., 1993, "Experimental Study about the Surface Roughness and Material Removal Rate of Ceramics Lapping," *Proceedings of the Korean Society of Precision Engineering Fall Annual Meeting* '93, pp. 131~135. (in Korean)

Ajayi, O. O. and Ludema, K. C., 1988, "Surface Damage of Structural Ceramics: Implications for Wear Modeling," *Wear*, Vol. 124, pp. 237~257.

Buijs, M. and Houten, K. K., 1993, "Three-body Abrasion of Brittle Materials as Studied by Lapping," *Wear*, Vol. 166, pp. 237~245.

Chauhan, R., 1992, Free Abrasive Machining of Ceramics, M. S. Thesis, Purdue University, p. 59.

Chauhan, R., Ahn, Y., Chandrasekar, S. and Farris, T. N., 1993, "Role of Indentation Fracture in Free Abrasive Machining of Ceramics," *Wear*, Vol. 162~164, pp. 246~257.

Cook, R. F. and Pharr, G. M., 1990, "Direct Observation and Analysis of Indentation Cracking in Glasses and Ceramics," *J. Am. Ceram. Soc.*, Vol. 73, No. 4, pp. 787~817.

Grimes, G. M., Phillips, K. and Wilshaw, T. R., 1977, "On the Mechanism of Material Removal by Free Abrasive Grinding of Glass and Fused Silica," *Wear*, Vol. 41, pp. 327~350.

Hill, R., 1985, *The Mathematical Theory of Plasticity*, Oxford Clarendon Press, Chap. V.

Imanaka, O., 1966, "Lapping Mechanisms of Glass - Especially on Roughness of Lapped Surface," *Annals of CIRP*, Vol. 13, pp. 227~233.

Lawn, B. R. and Wilshaw, R., 1975, "Review Indentation Fracture: Principles and Applications," *J. Mater. Sci.*, Vol. 10, pp. 2016~2024.

Marsh, D. M., 1964, "Plastic Flow in Glass," *Proc. Roy. Soc. Lond.*, Vol. A279, pp. 420~435.

Marshall, D. B., Evans, A. G., Khuri-Yakub, B. T., Tien, J. W. and Kimo, G. S., 1983, "The Nature of Machining Damage in Brittle Materials," *Proc. Roy. Soc. Lond.*, Vol. A385, pp. 461~475.

Venkartraman, S. and Wilson, J. R., 1988, "Modeling Univariate Populations with Johnson's Translation System-Description of the Fittr1 Software," *Research Memorandum*, No. 87~21, School of IE, Purdue University.